Effect of Metal Binding on the Conformation of Enterobactin. A Proton and Carbon-13 Nuclear Magnetic Resonance Study†

M. Llinás,* D. M. Wilson,‡ and J. B. Neilands

ABSTRACT: The conformations of enterobactin and its Ga^{3+} chelate dissolved in $(CD_3)_2SO$ have been characterized by ^1H and ^{13}C nmr. All the resonances were identified and, in particular, the ester and amide carbonyl peaks on the ^{13}C spectrum of the chelate could be distinguished by means of double irradiation techniques. On metal binding the shifts in the aromatic region are mainly related to effects at the catechol ligands, while the aliphatic resonances clearly reflect a major conformational change. The amide proton becomes drastically deshielded upon chelation suggesting a perturbation of its electronic state which is consistent with both molecular models of the chelate and theoretical calculations for nonplanar amide bonds. The ^1H and ^{13}C chemical shifts suggest that the energy barrier for amide torsion is decreased by conjugation of its carbonyl with the catecholate ring. Structural models for free and chelated enterobactin are derived on the basis of the seryl proton–proton spin couplings.

Enterobactin (enterochelin), from *Escherichia coli* and other enteric bacteria, is the cyclic triester of 2,3-dihydroxy-*N*-benzoyl-L-serine (Pollack and Neilands, 1970; O'Brien and Gibson, 1970) (Figure 1). It belongs to the microbial "high-affinity" ferric iron transport compounds described collectively as "siderochromes" (Neilands, 1973).

Ferric enterobactin exhibits the characteristic g = 4.3 electron spin resonance signal found in ferrichrome A and other "rhombic field" high-spin Fe^{3+} compounds (O'Brien *et al.*, 1971; Peisach *et al.*, 1971). Hexacoordination of a 3^+ ion by the three catechols releases six protons and affords a chelate which is a 3^- anion (Pollack and Neilands, 1970; O'Brien and Gibson, 1970).

Molecular models allow a number of conformational arrangements for enterobactin and its metal chelates. Both left- and right-handed coordination propellers around the metal center appear feasible. The circular dichroism of the ferric complex shows, however, that metal chelation is stereoselective (Neilands, 1972). Furthermore, mononuclear chelation requires a distortion of the amide bond planarity which, depending on the assumed model, forces the conventional[1] ω angle to assume values of up to $\sim 90°$. Although examples of nonplanar amide bonds are becoming rather common (Hallam and Jones, 1970; Winkler and Dunitz, 1971), in the case of natural polypeptides they usually represent perturbations of less than 15° from the planar configuration (Ramachandran and Sasisekharan, 1968). In enterobactin, a large torsional angle would imply a considerable energy expenditure for chelation as the rotational barrier for a secondary amide bond has been estimated to lie between 13 and 22 kcal per mol (Hallam and Jones, 1970; Winkler and Dunitz, 1971) which is difficult to reconcile with the high ($>10^{25}$) iron-binding constant this siderochrome exhibits (O'Brien *et al.*, 1971).

We have already reported (Llinás *et al.*, 1972a,b) a proton magnetic resonance (pmr)-derived conformation for the ferrichrome-type siderochromes which, in general, correlates well with the X-ray analysis of these compounds (Zalkin *et al.*, 1966). The simplicity of the enterobactin structure makes of it a suitable candidate for similar studies, especially since nuclear magnetic resonance (nmr) chemical shifts are most sensitive to the orientation of proximal unsaturated bonds, which are abundant in the molecule.

In this communication we present a proton and carbon-13 nmr study of the solution conformation of enterobactin and of its metal chelate. As with the ferrichromes, a diamagnetic ion (Ga^{3+}) was substituted for Fe^{3+} to avoid line broadening by the paramagnetic ion. Resonance assignments for the pmr spectra of enterobactin in $(CD_3)_2SO$ and $(CD_3)_2CO$ have been reported (Pollack and Neilands, 1970; O'Brien and Gibson, 1970).

Materials and Methods

Enterobactin and its monomeric unit were extracted from culture media of *Aerobacter aerogenes* 62-1 grown under low iron conditions, as described by Pollack and Neilands (1970). The Ga^{3+} chelate of the siderochrome was prepared by adding a slight excess of $GaCl_3$ to an aqueous ethanol solution of enterobactin and then neutralizing with either NaOH or LiOH to pH ~ 7.5. At this pH level, excess Ga^{3+} precipitates as the hydroxide forming a gel which is readily separated by centrifugation and filtration to leave the trialkali salt of the chelate in solution. Six equivalents of base was required per mole of chelate formed. After flash evaporation, the gallium enterobactin salt was dried and stored *in vacuo* over P_2O_5 until use. Since the chelate oxidizes readily, solutions were prepared immediately prior to their spectra being taken.

The nmr data are for samples dissolved in $(CD_3)_2SO$ in 5-mm tubes. While concentrations ranging between 15 and 20 mg per 0.5 cm^3 were satisfactory for single-scan pmr spectra, up to 65 mg of sample were used in some ^{13}C magnetic resonance

† From the Departments of Biochemistry and Chemistry, University of California, Berkeley, California 94720. *Received April 4, 1973.* Sponsored by a U. S. Public Health Grant No. A104156 and a National Science Foundation Grant No. GB5276X. A preliminary communication of this investigation has been reported elsewhere [Llinás, M., Wilson, D. M., and Neilands, J. B., *Fed. Proc., Fed. Amer. Soc. Exp. Biol. 31*, Abstr. 3782 (1972)].

‡ Present address: Space Sciences Laboratory, University of California, Berkeley, Calif. 94720.

[1] Throughout this paper, the structural description follows the nomenclature and conventions proposed by the IUPAC-IUB Commission on Biochemical Literature for polypeptides [*J. Mol. Biol. 52*, 1 (1970)]. Here, however, $\psi = 0$ is defined for that conformation where the amide nitrogen eclipses the ester β oxygen along the C_α–C′ bond.

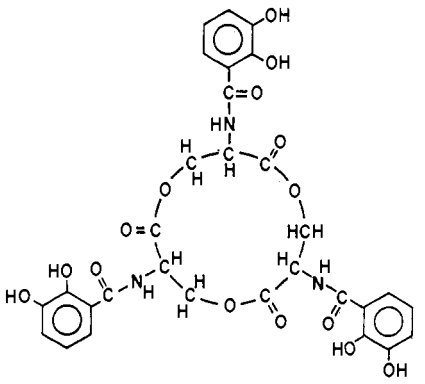

FIGURE 1: Enterobactin. Three L-seryl residues are head to-tail ester bonded to form a cyclic trimer. The amino groups form, in turn, amide bonds with 2,3-dihydroxybenzoic acid which provides the catechol ligands that coordinate the metal.

(cmr) experiments. Me_4Si and *p*-dioxane were used as internal reference for the proton and carbon-13 spectra, which were taken on spectrometers operating at 220 MHz (Varian HR-220) and 14 kG (Varian HR-60), respectively. The latter was modified for high-resolution pulsed Fourier transform spectroscopy and was provided with external ^7Li lock and ^1H coherent or noise decoupler. An earlier version of this spectrometer has been described elsewhere (Horsley *et al.*, 1970). From 11,000 to 50,000 free induction decays per spectrum were accumulated on a Fabri-Tek 1074 signal averager with 4096 word memory, transferred to magnetic tape, and numerically Fourier transformed by the CDC 6600 computer of the Lawrence Berkeley Laboratory.

Results and Discussion

The structural implications of the pmr spectra of enterobactin and its Ga^{3+} chelate will be analyzed first. The cmr data will then be presented and used to support the interpretation of the pmr results. Conformational models for the free and complexed siderochrome will be proposed.

Pmr Evidence. The 220-MHz pmr spectra of enterobactin and its Ga^{3+} chelate, dissolved in $(CD_3)_2SO$ at ~43°, are shown in Figure 2. The chemical shifts (δ) of the resonances as well as the proton–proton spin coupling constants (J) are given in Tables I and II, respectively. The two low-field bands (at 11.57 and 9.34 ppm) in the enterobactin spectrum, which lack multiplet structure, are assigned to the catechol hydroxyls (Figure 2a). They disappear upon metal binding (Figure 2b) and vanish rapidly in the presence of D_2O, the fast exchange with residual water accounting for their not being detected by earlier investigators (Pollack and Neilands, 1970; O'Brien and Gibson, 1970). These resonances are separated by 2.13 ppm (Table I). Salicylaldehyde is known to have the *o*-phenol H bonded to the carbonyl oxygen (see *e.g.*, Vinogradov and Linnell, 1971). In enterobactin such an H bond should be even stronger as the proton acceptor group is relatively more electronegative because of its participation in an amide bond. Moreover, the possibility of conjugation of the phenolate with the carbonyl would result in a higher intrinsic acidity of the ortho relative to the meta hydroxyl while further strengthening the intramolecular H bond. Thus, *a priori* one would expect the ortho phenol to be electronically more deshielded than the homologous meta proton while being more stabilized toward chemical exchange because of the intramolecular H bond. The latter would narrow the low-field resonance line, which is indeed observed in this spectrum.

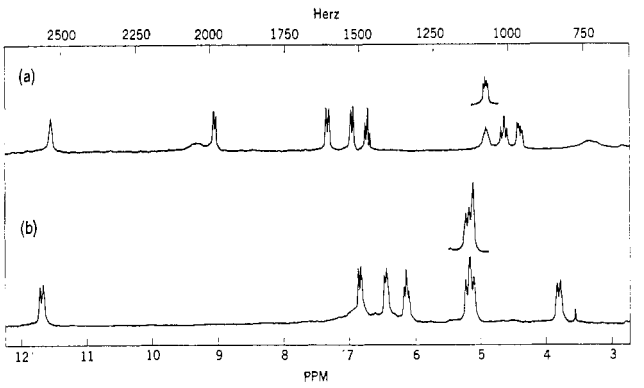

FIGURE 2: The 220-MHz pmr spectra of enterobactin (a) and Ga^{3+}-enterobactin (b) dissolved in $(CD_3)_2SO$ at ~45°. Chemical shifts are referred to internal Me_4Si and are listed in Table I. Inserts above each spectrum show the α-proton resonance after the amide has been exchanged with D_2O. See Table II for the magnitudes of the proton spin–spin coupling constants (J). The broad resonance *ca.* 3.4 ppm is due to residual water.

The amide link between the seryl-α-amino and the benzoyl carboxylate should be expected to be trans in enterobactin as there are no steric reasons to obstruct this energetically favored configuration (Hallam and Jones, 1970). Furthermore, the phenol–carbonyl H bond and the feasibility of resonance conjugation between amide and the benzenoid ring, discussed above, should somewhat lower the energy of an amide–benzoyl planar configuration.

A related effect is the rather low-field position of the seryl NH resonance. At ~45° a peptide amide NH exposed to $(CD_3)_2SO$ is typically observed between 7.5 and 8.4 ppm (Llinás *et al.*, 1972a) which should be contrasted with the 9.08 ppm observed in enterobactin. This is ascribed partly to a "ring current" deshielding from the benzenoid group, as the amide proton is ~3.6 Å from the ring center on its equatorial plane (Haigh and Mallion, 1972), and partly to the ortho phenol H-bond stabilization of the carbonyl electron density, which enhances the acidity of the amide dipole.

TABLE I: Pmr Chemical Shifts.[a]

Proton	Enterobactin	Ga^{3+}-enterobactin
	Benzoyl	
o,p-CH	7.34, 6.98	6.84, 6.44
m-CH	6.73	6.13
o-OH	11.56	
m-OH	9.34	
	Seryl	
$C_\alpha H$	4.94	5.14
$C_\beta H_1$	4.66	5.22
$C_\beta H_2$	4.41	3.80
NH	9.06 (−4.73)	11.72 (−1.32)

[a] The pmr chemical shifts (parts per million), referred to internal Me_4Si, of enterobactin and its Ga^{3+} chelate in $(CD_3)_2SO$ at ~45° and 220 MHz. $C_\beta H_1$ and $C_\beta H_2$ shifts refer to β protons in the order they resonate in scanning from low to high field and do not imply absolute assignment or correspondence between the free and metal-bound siderochrome. The slopes of the amide NH chemical shift *vs.* temperature linear plots are shown in parentheses in units of ppm/°C, multiplied by 10^3.

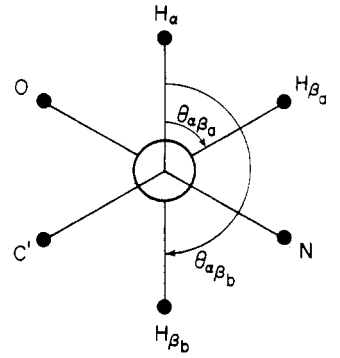

FIGURE 3: Dihedral angles (θ) between the α and β protons. For illustrative purposes the Newman projection shown here depicts a fully staggered conformation ($\theta_{\alpha\beta_a} = 60°$, $\theta_{\alpha\beta_b} = 180°$) which does not correspond to either enterobactin or its Ga^{3+} complex. Angles for the latter are given in the text and in the legends to Figure 4 and 7, respectively. It should be noted that the value for the conventional dihedral angle χ is directly given by $\theta_{\alpha\beta_b}$.

A result of postulating coplanarity of the free catechol and amide groups is that once the conformation of the enterobactin seryl triester backbone is elucidated, only one degree of freedom (about the C_α–N bond) remains. CPK space-filling and Dreiding models can then be employed to simulate steric hindrances and bond geometry constraints, respectively, of plausible structures.

The seryl α-proton resonance at 4.94 ppm is readily identified since it is simplified to a composite of two neatly resolved doublets (J = 4.19, 8.06 Hz) upon exchange of its spin–spin-coupled α-amino proton by deuterium (Figure 2a). The two resonances which follow toward higher fields, at 4.66 ppm (J = 8.06 Hz) and 4.41 ppm (J = 4.19 Hz), are unaffected by the exchange and are assigned to the two seryl β protons. Similarly, in gallium enterobactin the J = 9.83 Hz doublet at 5.14 ppm is identified as arising from the α proton while the two J = 10.68 Hz doublets at 5.22 and 3.80 ppm are assigned to the vicinal β protons (Figure 2b). Conformational information is contained in the chemical shifts as well as in the proton–proton spin interactions. These two criteria immediately indicate (Tables I and II) that while a significant conformational change accompanies metal chelation, C_3 symmetry is maintained.

Conformation of Enterobactin. Equations of the type

$$\begin{cases} J(\theta) = k_1 \cos^2(\theta) - c & \text{for} \quad |\theta| \leq 90° \\ J(\theta) = k_2 \cos^2(\theta) - c & \text{for} \quad 90° \leq |\theta| \leq 180° \end{cases} \tag{1}$$

have been proposed to relate spin–spin coupling constants between vicinal protons and the absolute dihedral angle between them along the C–C bond (see, *e.g.*, Sternhell, 1969). In our case, the two criteria that an acceptable $\{k_1, k_2, c\}$ set must fulfill are: (a) it should be equally valid for calculations on enterobactin and on its gallium chelate, and (b) calculated angles between the α and each of the β protons should differ by about 120° (the projected sp^3 hybridization bond angle). The lack of observable multiplicity at the α proton resonance in the chelate after exchanging the amide with D_2O (Figure 2b) means that the sum of the two α–β couplings is minimal, *i.e.*, of the order of, or less than, its line width (~3 Hz). On the basis of relationships (1) and accounting for criterion (b), such small splitting can be satisfied either by $\theta_{\alpha\beta_a} = -\theta_{\alpha\beta_b} \cong -60°$, or by $\theta_{\alpha\beta_a} \cong 120° = \theta_{\alpha\beta_b} - 120°$. For steric reasons,

TABLE II: Proton–Proton Spin Couplings.[a]

Doublet	Enterobactin	Ga^{3+}-enterobactin
o-m, *p-m*	8.02, 7.75	7.36, 6.41
o-OH	None	
m-OH	None	
α-β_1	8.06	Unresolved
α-β_2	4.19	Unresolved
β_1-β_2	10.80	10.68
α-N	6.52	9.83

[a] J coupling constants for the proton spin–spin interactions in enterobactin and its Ga^{3+} complex. The values are in hertz and were directly measured on expanded-scale spectra. The aryl *o-m* and *p-m* splittings in the chelate might be underestimated because of broadening of the resonances.

the second set of angles has to be discarded as it results in serious pressures among the three β_b hydrogens in attempting to fit them at the center of any CPK model that respects C_3 symmetry. The ±60° set of angles is otherwise more satisfactory in that it yields an absolute minimum for the $J_{\alpha\beta_a} + J_{\alpha\beta_b}$ sum (henceforth ΣJ_{min}). From theory, Karplus has derived that k_1 = 8.5 Hz, k_2 = 9.5 Hz, and c = 0.28 Hz (Karplus, 1959). Unfortunately, these values are affected by the electronegativity of the substituents attached to the pertinent carbon atoms (Sternhell, 1969; Karplus, 1963). A novel approach for finding an acceptable set of Karplus parameters has been proposed by Slessor and Tracey (1971). The procedure has been termed "Dihedral Angle Estimation by the Ratio Method" (DAERM). It is assumed that c = 0.28 Hz and that a satisfactory set of k_1 and k_2 should yield k_1/k_2 = 0.9, which is the ratio value for the theoretical parameters. Dihedral angles can thus be estimated for hydrogens vicinal to a methylene function without consideration of the inductive effects acting on the system, but only on the basis of relationships (1) and the ratio $(J_{\alpha\beta_a} + c)/(J_{\alpha\beta_b} + c)$ calculated from the experimentally determined couplings. However, besides accurately measured J's, DAERM also requires, for certain angular regions, unequivocal assignment of the resonances to the corresponding H_{β_a} and H_{β_b} (*i.e.*, it requires knowledge as to whether an α–β doublet arises from H_α–H_{β_a} or from H_α–H_{β_b} couplings, see Figure 3). Although this was not possible from our data, it so happens that independently of the assignment of the enterobactin individual β resonances, only angles in the range $\theta_{\alpha\beta_a} < 90°$, $\theta_{\alpha\beta_b} = \theta_{\alpha\beta_a} + 120° > 90°$ yield satisfactory values for k_1 and k_2 in terms of criterion (a). This is totally unequivocal as for other ranges in the θ's the k_i's that result are excessively large (>20 Hz). Of the two possibilities, attributing H_{β_2} ($J_{\alpha\beta_2}$ = 4.19 Hz) to H_{β_a} and H_{β_1} ($J_{\alpha\beta_1}$ = 8.06 Hz) to H_{β_b} yields parameter values (k_1 = 8.12 Hz, k_2 = 9.19 Hz) that minimize ΣJ_{min} (= 1.75 Hz) more than the alternate assignment (→ k_1 = 8.96 Hz, k_2 = 9.16 Hz, ΣJ_{min} = 1.96 Hz). Without sufficient spectral resolution to decide between the two alternatives, we arbitrarily choose the former assignment over the latter. The dihedral angles obtained for the α–β protons on the basis of the selected set of parameters and eq 1 yield $\theta_{\alpha\beta_a}$ = 42°, and $\theta_{\alpha\beta_b}$ = 162° when viewed from the α end of the C_α–C_β axis (Figure 3). The alternate assignment yields $\theta_{\alpha\beta_a}$ = 13°, $\theta_{\alpha\beta_b}$ = 133°, *i.e.*, it does not modify the proposed structure significantly.

Having arrived at a seryl side-chain conformation does not define the relative orientation of the ester group. Space-filling

SCHEME I

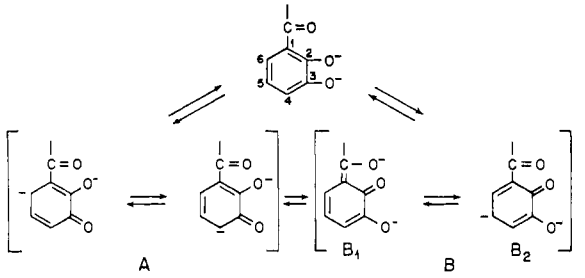

models show that the ester group can be basically oriented with the carbonyl pointing either "up" or "down" from a plane bisecting the cyclic backbone. As can be judged from the chemical differences between their resonances the two β protons are relatively more equivalent (in the pmr sense) in the free ligand than in the chelate (Figure 2a,b). This would suggest that the orientation of the carbonyls at the ester and amide bonds should be such that the anisotropic shifts they generate on the enterobactin β protons be similar and small. The structure proposed in Figure 4 results in such shifts, as the β_a and β_b protons are both situated near the nodal (zero shift) regions of the two π systems.

CPK molecular models show considerable steric hindrance for rotation of the planar benzoyl amide around the N–C_α bond since it tightly fits in the space limited by the ester group and the β hydrogens (Figure 4). Hence, either a cis (θ_{NC} = 0° → ϕ = 60°) or a *trans* (θ_{NC} = 180° → ϕ = −120°) configuration is suggested for this bond. A decision can be reached on the basis of the vicinal NH–C_αH proton spin–spin coupling constant, measured to be J_{NC} = 6.52 Hz (Table II). Indeed, using the most recent Karplus relationship proposed for this type of coupling (Ramachandran *et al.*, 1971), namely

$$J_{NC} = 7.9\cos^2\theta - 1.5\cos\theta + 1.3\sin^2\theta \qquad (2)$$

(in hertz units, estimated electronegativity corrections included), $\theta_{NC} \cong 0°$ (→ $J_{NC} \cong 6.4$ Hz) is indicated as the favored dihedral angle and is that shown in the model (Figure 4).

State of the Ligands. Upon metal binding there is an excess of one minus charge per benzene ring to be delocalized with ortho, para preference. The tautomers in Scheme I may thus be drawn. Resonances of this type might be responsible for the exchange lability of the phenylalanyl ϵ hydrogens (ortho to the phenol) (Cohen and Putter, 1970).

Brown (1964) has shown that the electron delocalization in phenoxides is very much reduced when the charge is stabilized on the oxygen atom by, *e.g.*, H bonding to the solvent or extensive ion pairing with the cation. A similar charge stabilization mechanism has recently been suggested to explain the optical spectral differences between free and metal-complexed phenoxides in the transferrins (Teuwissen *et al.*, 1972). We propose that such is the case in coordinated enterobactin and that the favored charge distribution places more electron density on the meta than on the ortho oxygen atom. Forms B expand the conjugation to the carbonyl. In particular, tautomer B_1 achieves maximal separation between the two electrons and exposes the negatively charged carbonyl to the solvated counterion. Thus, on going from enterobactin to its Ga^{3+} complex the aryl proton resonance that shifts the most ($\Delta\delta$ = −0.6 ppm) is the meta triplet (attached to C_5), rather than the ortho or para doublets (attached to C_6 and C_4, $\Delta\delta$ = −0.5 and −0.54 ppm), while the overall shifts indicate loss in

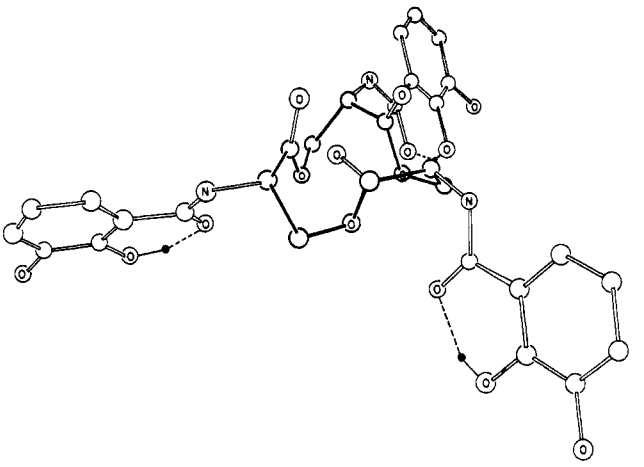

FIGURE 4: Molecular model for enterobactin dissolved in dimethyl sulfoxide. The cyclo ester backbone atoms and bonds are shown in heavier lines. No hydrogen atoms are depicted except for the strongly H-bonded ortho phenolic group. Assuming planarity of the benzoyl amide moiety (ω = 180°), the three dihedral angles that characterize the model are: $\phi \cong 60°$, $\psi \cong 100°$, and $\chi \cong 162°$.

aromaticity as would be expected for the semiquinoid tautomers. The similarity between the latter

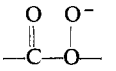

and the hydroxamate

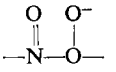

function found in the ferrichromes is compatible with the common biological role of these compounds (Luckey *et al.*, 1972). Furthermore, unsaturated cyclic keto enolic groups of this type are found in the antibiotic kojic acid and in the tropolones, both natural products with strong iron-binding affinities (Sillén and Martell, 1964, 1971).

Related to the phenol–carbonyl conjugation is the extreme low field shift of the NH resonance on going from enterobactin to its gallium chelate ($\Delta\delta$ = +2.66 ppm). Titration of enterobactin with NaOH (both dissolved in $(CD_3)_2SO$) results in a pronounced deshielding of the amide as the titration proceeds and a downfield shift of ~1.55 ppm could be observed before the signal disappeared by broadening (base-catalyzed H exchange). Such deshielding reflects a change in the electronic state of the amide bond, as in tautomer B_1 (Scheme I), reducing the amine–carbonyl resonance responsible for amide planarity

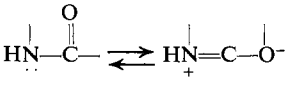

so that rotation around this bond becomes possible. Indeed, rigorous LCAO–MO calculations by Yan *et al.* (1970) have indicated an increase in positive charge at the amine hydrogen as an amide bond is rotated from a planar cis or trans configuration to 90°. This is of immediate significance as it provides a clue to understanding the conformational stability of the chelate in spite of the unusual amide bond torsion required for its formation.

Cmr Evidence. The cmr spectra of 2,3-dihydroxy-*N*-benzoyl-L-serine (free acid), enterobactin, and Ga^{3+}-enterobactin, are shown in Figure 5A, B, and C, respectively. The reso-

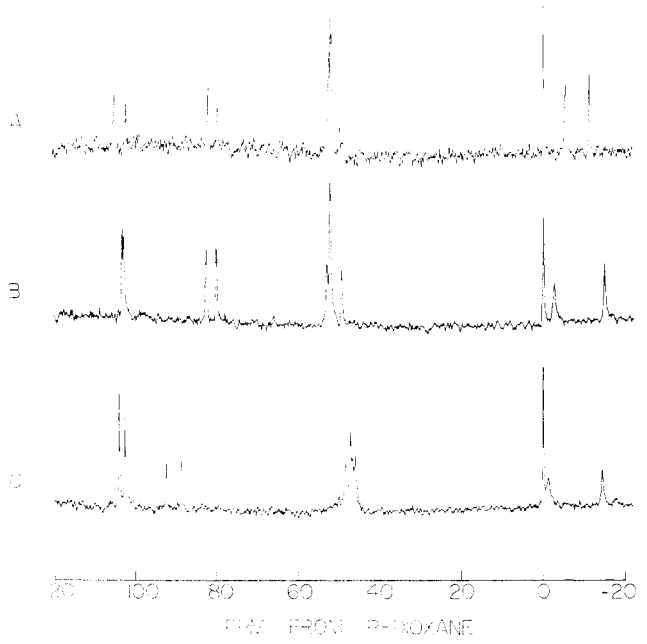

FIGURE 5: Carbon-13 nmr proton noise-decoupled spectra of enterobactin monomer (2,3-dihydroxy-*N*-benzoyl-L-serine) (A), free enterobactin (B), and Ga^{3+}-enterobactin (C), for the compounds dissolved in $(CD_3)_2SO$ at ~50°. Chemical shifts are referred to internal *p*-dioxane. From 17,000 to 49,000 free-induction decays following 40° nutation pulses at 1.6-sec intervals were accumulated at a 10-kHz A/D rate and Fourier transformed.

nances are readily identifiable and most are assignable to particular carbon atoms (Table III).

The transition from the (acid) monomeric species to free enterobactin broadens the ^{13}C resonances, consistent with a decrease in motional freedom. Comparison of spectra A and B enables assignment of the seryl resonances as these shift the most upon formation of the cyclic trimer. In spectrum A, the two peaks to higher field from the dioxane reference are attributed to the seryl β and α carbons, in order of increasing shielding (Horsley *et al.*, 1970). According to Lippmaa and Pehk [cited in (Stothers, 1972a)], esterification shifts the "acid-side" α- and β-carbon resonances to high and low fields, respectively, while the corresponding carbons on the "alcohol side" move in opposition. In enterobactin, the seryl α and β carbons are α and β relative to the C′ carbonyl but are β and α relative to the hydroxyl end, so that in forming the trimer the effects on the amino acid α and β carbons are additive. This rationalization predicts that the peaks at −2.7 and −14.9 ppm in the enterobactin spectrum (Figure 5B) should be assigned to the seryl β and α carbons, respectively, which was confirmed by off-resonance coherent proton decoupling experiments. Similarly, the transition from the monomer to the triester identifies the two low-field enterobactin resonances, barely resolved at 102.5 and 102.9 ppm, as arising from the amide and ester carbonyls, respectively.

It can be deduced from the reported spectra of phenol and cathechol (Johnson and Jankowski, 1972) that the two peaks at 82.3 and 79.8 ppm correspond to the two oxygen-bound phenolate carbons while the group centered at about 52 ppm belongs to the remaining four aryl atoms (Figure 5A,B). In the absence of more precise information, the effect of an amide substituent on the catechol carbon shieldings may be roughly estimated from the shifts induced by a methyl ester group on the benzene carbon resonances (Stothers, 1972b). This approach indicates that the two aryl ^{13}COH's should exhibit similar chemical shifts as the methyl ester substituent affects benzyl ortho and meta carbons to the same extent (−0.3 ppm). In a study of H-bonding effect on phenolic ^{13}C resonances, Maciel and James (1964) have found that the stronger the H-bond acceptor nature of the solvent, the greater the ^{13}COH resonance shifts to lower fields, approaching, in the limit, the position of a fully ionized phenolate at about 9.8 ppm downfield from dimethyl sulfoxide dissolved (*i.e.*, H-bonded) phenol. The low-field move caused by increased solvent basicity has been attributed by the authors to a displacement of the equilibria

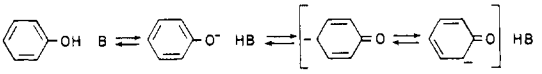

to the right. Thus, instead of shifting towards the $^{13}CO^-$ position, the ^{13}COH resonance becomes even more deshielded because of the semiquinoid $^{13}C{=}O$ tautomer form with which it is in equilibrium (*e.g.*, $^{13}C{=}O$ in benzoquinone resonates at 119.7 ppm from dioxane (Johnson and Jankowski, 1972), or at about 19.8 ppm from fully ionized phenolate). This trend suggests that in enterobactin the 2.5-ppm difference between the two oxygen-bound catechol carbon resonances might be due to intramolecular H bonding of the ortho ^-OH to the amide carbonyl, in agreement with the pmr data. The low-field position of the amide $^{13}C{=}O$ resonance might also be attributed to this effect since otherwise carbonyls attached to aromatic rings are known to be relatively shielded (Stothers, 1972c). Furthermore, the catechol carbon resonances shift to lower field about 9.25 ppm, on going from enterobactin to the chelate (Figure 5B,C, Table III) while the relative shift between the two oxygen-bound ^{13}C resonances increases from 2.5 ppm in enterobactin to 3.6 ppm in the chelate. Since the absence of intramolecular H bonding in the chelate would dictate the opposite effect, *i.e.*, a closer magnetic equivalence of these carbons, clearly another mechanism exists. Employing semiquinoid structural analogies means that in gallium enterobactin the two carbon atoms in question are not π bonded to oxygen to the same extent, supporting our contention that canonical forms A and B (Scheme I) are not equally favored. It

TABLE III: Cmr Chemical Shifts.[a]

Carbon	Monomer	Enterobactin	Ga^{3+}-enterobactin
–COO–	105.0	102.9	103.7
–CONH–	102.1	102.5	102.3
o-COH	82.0	82.3	92.1
m-COH	79.6	79.8	88.5
$-C_iH$	52.4	52.8	48.3
$-C_4H$	52.1	52.0	47.2
$-C_5H$	51.8	52.0	46.8
$-C_6H$	49.8	49.2	46.0
$-C_\beta H_2O-$	−5.3	−2.7	−1.2
$-C_\alpha HNH-$	−11.2	−14.9	−14.4

[a] Carbon-13 nmr chemical shifts (±0.1 ppm, referred to internal *p*-dioxane) of 2,3-dihydroxy-*N*-benzoyl-L-serine (acid monomer), enterobactin, and Ga^{3+}-enterobactin, in $(CD_3)_2SO$ at ~50°C. C_iH refer to hydrogen-bound aryl ^{13}C atoms in the order they resonate from low to high field and do not imply either absolute assignment or correspondence among the three compounds.

should be noted that the overall shift of these two ^{13}C resonances concomitant to chelation is more extensive than the moves observed upon cation binding in several natural and artificial alkali complexones (Ohnishi *et al.*, 1972; Bystrov *et al.*, 1972; Pretsch *et al.*, 1972). In case of the latter compounds, metal binding is by ion–dipole interaction and the resonance shifts should be accounted for mainly by an electronic mobilization along the C=O bond toward the coordinated ion. This is not strictly the case with enterobactin, where the ion–siderochrome interaction is by ion–ion pairing, and more than enough negative charge is available in the fully ionized catecholate. Thus, on coordinating Ga^{3+}, an electron density gain in the catechol ring is apparent as the cluster of the C_1, C_4, C_5, and C_6 aryl resonances shifts ~ -3.85 ppm, further supporting the proposed increased electron delocalization in the chelate.

In a cmr study of valinomycin, it has been proposed that ester and amide carbonyl peaks should be distinguishable by their widths since a next-to-nitrogen $^{13}C{=}O$ should exhibit resonances broader than a next-to-oxygen homolog because of the ^{14}N relaxation effects (Ohnishi *et al.*, 1972). Here a more direct identification was attempted using a selective decoupling technique. Figure 6 shows the $^{13}C{=}O$ resonance region of the Ga^{3+}-enterobactin spectrum taken under identical conditions except for the characteristics of the proton decoupling, which were: no decoupling (A), weak coherent decoupling of the amide proton (B), weak coherent decoupling of the seryl α and β protons (C), and strong noise decoupling (D). Using the formulation of Ernst (1966), the weak decoupling radiofrequency field strength H_2 was estimated to be 95 mG by means of the real and apparent $^{13}C_\alpha$–$^1H_\alpha$ J couplings under conditions of no proton irradiation and amide proton decoupling, respectively. Comparison of Figure 6B and 6C with 6A shows that although substantial nuclear Overhauser enhancement of both carbonyls resulted from the weak decoupling regardless of its frequency relative to the proton spectrum, the upfield carbonyl does not share a J coupling constant of more than *ca.* 4 Hz with any proton, while the downfield carbonyl shares a larger coupling constant with one or more non-amide protons. The enterobactin primary structure allows one geminal and four vicinal non-amide couplings of the trimer ester carbonyl to protons, some of which would be expected to be at least 6 Hz (Stothers, 1972d; Jameson and Damasco, 1970; Schwarcz and Perlin, 1972). The amide (benzoyl) carbonyl has only two non-amide interactions, vicinal couplings to the C_α proton and to the benzoyl ortho proton, which may be estimated from studies of *N,N*-dimethyl acetamide (Gray *et al.*, 1969) and methyl benzoate (Ihrig and Marshall, 1972) to be *ca.* 3 and 4 Hz, respectively. Thus Figure 6 suggests assignment to the downfield and upfield carbonyl resonances to the trimer ester and amide (benzoyl) carbonyls, respectively.

The overall insensitivity of the benzoyl $^{13}C{=}O$ resonance to the charge delocalization effects in the metal-bound catecholate contrasts with the significant shift detected in the pmr of the amide NH (Figure 2). This is, however, easily rationalized given the known facility (Stothers, 1972c) with which the hole on the carbonyl dipole delocalizes toward conjugated electron donor groups, namely, the amide nitrogen in enterobactin and the catecholate ring in the complex. Even if removal of the H bonding and a drop in ring current deshieldings should be expected for the chelate benzoyl carbonyl, according to the theoretical calculations already mentioned (Yan *et al.*, 1970) an opposing reduction in electron density at the participating C=O should be expected upon torsion of the amide from the planar configuration. The shifts of the ester backbone α, β, and C′ resonances ($\Delta\delta = -0.5$, -1.5, and -0.8 ppm, respectively) should be attributed to conformational effects and further exemplify the ability of cmr to detect such changes. C_3 symmetry is again indicated for the free and metal-bound enterobactin by the ^{13}C spectra.

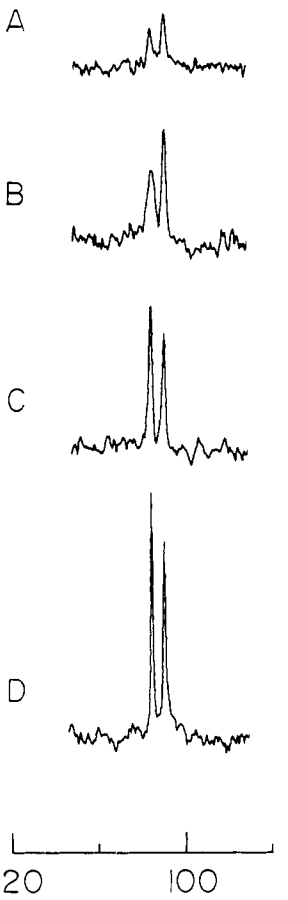

FIGURE 6: Carbonyl region cmr of enterobactin complexed to Ga^{3+}: (A) no proton decoupling, (B) amide proton (11.72 ppm from Me_4Si in the proton spectrum) coherently decoupled at low power, (C) α-proton (5.14 ppm from Me_4Si in proton spectrum) coherently decoupled at low power, and (D) all protons noise decoupled at high power.

Conformation of Ga^{3+}-enterobactin. The C_α–C_β configuration for the chelate has been established as defined by $\theta_{\alpha\beta_b} \cong -\theta_{\alpha\beta_a} \cong 60°$. However, molecular models indicate that, these angles fixed, both left- and right-handed propellers can be generated around the metal without stressing the structure. Of the two, the left-handed configuration (the same present in the ferrichromes) might be favored since it places the β_b proton into closer interaction with the unsaturated amide–catechol system (see below). This choice needs further substantiation. With this single reservation, the model we favor is shown in Figure 7. As in enterobactin, it would also appear possible to have the ester carbonyls pointing down from the cyclic backbone. Space-filling models indicate excessive crowding of the carbonyl oxygen atoms at the molecular axis above the metallic complex center in this arrangement and it should hence be discarded.

The extreme chemical shift difference between the two β protons in the chelate ($\Delta\delta = 1.42$ ppm) relative to enterobactin ($\Delta\delta = 0.28$ ppm) can be explained by the models as in the former the β_b hydrogen lies between the unsaturated benzoyl π system and the ester carbonyl while the geminal β_a (pointing axially into the cycloester ring) would suffer neg-

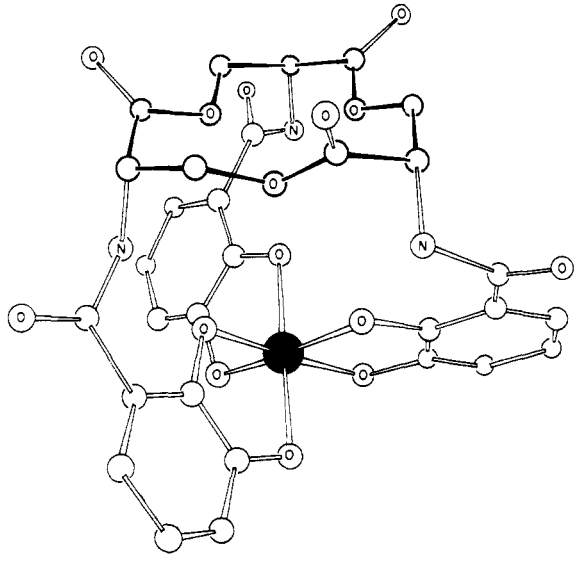

FIGURE 7: Molecular model for Ga^{3+}-enterobactin. The diagram follows the same conventions as that in Figure 4, with which it should be compared. The four dihedral angles that characterize the model are: $\phi \cong -150°$, $\psi \cong 100°$, $\omega \cong -133°$, and $\chi \cong 60°$.

ligible deshielding from the two neighbor C′ carbonyls. As observed in the ferrichromes, exaggeration of anisotropic effects are expected in the chelate relative to enterobactin because of the conformational stability enforced by coordination of the metal. This might indeed be the explanation for the small (0.21 ppm) shift of the H_α resonance upon chelation, since the position of this proton relative to the C′ carbonyl ($\psi \sim 100°$) is unaffected by the proposed conformational change.

It is further suggested that no unusual strained situation prevails in the gallium complex as the geminal coupling constants between the seryl β protons do not differ significantly on going from the free to the chelated state. Also, the aryl ring structure comfortably assumes a flat benzoyl disposition, *i.e.*, with the benzoyl C=O lying on the benzene plane. The distortion of the amide planarity by ~47° from the trans configuration is such that the N–H bond becomes oriented away from the solvent and towards the metal-binding center, critically avoiding steric crowding between the hydrogen and the (chelated) phenoxide ortho oxygen atom. Since no significant retardation of the amide hydrogen–deuterium exchange was observed upon addition of trace amounts of D_2O to the dimethyl sulfoxide solution, it is suggested that the amide is not appreciably H bonded to the phenolate oxygen. Some protection of this amide hydrogen upon complexation is indicated, however, since the temperature dependence of the proton chemical shift drops from -4.73×10^{-3} ppm/°K in enterobactin to -1.31×10^{-3} ppm/°K in the chelate (Table II), in agreement with the decreased exposure it exhibits in the model. Finally, the rather large dihedral angle between H_α and H_N ($\theta \sim 150° \rightarrow \phi \sim -150°$) is consistent with the large J_{NC} observed. It should be noted that direct application of relationship (2) to estimate the dihedral angle is not granted if, as argued above, the electronic configuration of the amide bond has been affected.

The model for the chelate shows exposure of the seryl $H_{\beta b}$, which is the one that becomes substituted by a methyl group on going from L-serine to L-threonine. Teleologically, this is satisfying since 2,3-dihydroxybenzoylthreonine has been isolated from cultures of *Klebsiella oxytoca* (Korth, 1970).

It would be gratifying if the conformational changes revealed by the nmr spectra of enterobactin and its chelates sheds some light on the mechanism of its carrier function and on its Fe-dependent susceptibility to cleavage by microbial esterases (Bryce and Brot, 1972; Langman *et al.*, 1972; Porra *et al.*, 1972).

Acknowledgments

The authors are indebted to Dr. E. J. Wawszkiewics for the *A. aerogenes* 62-1 culture, which was from the collection of Dr. F. Gibson, and to Dr. M. P. Klein for the use of the Varian HR-220 spectrometer and computational facilities.

References

Brown, J. M. (1964), *Tetrahedron Lett. 32*, 2215.
Bryce, G. F., and Brot, N. (1972), *Biochemistry 11*, 1708.
Bystrov, V. F., Ivanov, V. T., Kozmin, S. A., Mikhaleva, I. I., Khalilulina, K. K., and Ovchinnikov, Y. A. (1972), *FEBS (Fed. Eur. Biochem. Soc.) Lett. 21*, 34.
Cohen, J. S., and Putter, I. (1970), *Biochim. Biophys. Acta 222*, 515.
Ernst, R. R. (1966), *J. Chem. Phys. 45*, 3845.
Gray, G. A., Ellis, P. D., Traficante, D. D., and Maciel, G. E. (1969), *J. Magn. Resonance 1*, 41.
Haigh, C. W., and Mallion, R. B. (1972), *Org. Magn. Resonance 4*, 203.
Hallam, H. E., and Jones, C. M. (1970), *J. Mol. Structure 5*, 1.
Horsley, W., Sternlicht, H., and Cohen, J. S. (1970), *J. Amer. Chem. Soc. 92*, 680.
Ihrig, A. M., and Marshall, J. L. (1972), *J. Amer. Chem. Soc. 94*, 3268.
Jameson, C. J., and Damasco, M. C. (1970), *Mol. Phys. 18*, 491.
Johnson, L. F., and Jankowski, W. C. (1972), Carbon-13 NMR Spectra, New York, N. Y., Wiley.
Karplus, M. (1959), *J. Chem. Phys. 30*, 11.
Karplus, M. (1963), *J. Amer. Chem. Soc. 85*, 2870.
Korth, H. (1970), *Arch. Mikrobiol. 70*, 297.
Langman, L., Young, I. G., Frost, G. E., Rosenberg, H., and Gibson, F. (1972), *J. Bacteriol. 112*, 1142.
Llinás, M., Klein, M. P., Neilands, J. B. (1972a), *Int. J. Peptide Protein Res. 4*, 157.
Llinás, M., Klein, M. P., and Neilands, J. B. (1972b), *J. Mol. Biol. 68*, 265.
Luckey, M., Pollack, J. R., Wayne, R., Ames, B. N., and Neilands, J. B. (1972), *J. Bacteriol. 111*, 731.
Maciel, G. E., and James, R. V. (1964), *J. Amer. Chem. Soc. 86*, 2893.
Neilands, J. B. (1972), *in* Structure and Function of Oxidation Reduction Enzymes, Åkeson, Å., and Ehrenberg, Å., Ed., New York, N. Y., Pergamon Press, pp 541–547.
Neilands, J. B. (1973), *in* Inorganic Biochemistry, Vol. I, Eichhorn, G., Ed., New York, N. Y., Elsevier, pp 167–202.
O'Brien, I. G., Cox, G. B., and Gibson, F. (1971), *Biochim. Biophys. Acta 237*, 537.
O'Brien, I. G., and Gibson, F. (1970), *Biochim. Biophys. Acta 215*, 393.
Ohnishi, M., Fedarko, M. C., Baldeschweieler, J. D., and Johnson, L. F. (1972), *Biochem. Biophys. Res. Commun. 46*, 312.
Peisach, J., Blumberg, W. E., Lode, E. T., and Coon, M. J. (1971), *J. Biol. Chem. 246*, 5877.
Pollack, J. R., and Neilands, J. B. (1970), *Biochem. Biophys.*

Res. Commun. 38, 989.
Porra, R. J., Langman, L., Young, I. G., and Gibson, F. (1972), *Arch. Biochem. Biophys. 153*, 74.
Pretsch, E., Vasák, M., and Simon, W. (1972), *Helv. Chim. Acta 55*, 1098.
Ramachandran, G. N., Chandrasekaran, R., and Kopple, K. D. (1971), *Biopolymers 10*, 2113.
Ramachandran, G. N., and Sasisekharan, V. (1968), *Advan. Protein Chem. 23*, 283.
Schwarcz, J. A., and Perlin, A. S. (1972), *Can. J. Chem. 50*, 3667.
Sillén, L. G., and Martell, A. E. (1964), Stability Constants of Metal-Ion Complexes, London, The Chemical Society, pp 473–474.
Sillén, L. G., and Martell, A. E. (1971), Stability Constants of Metal-Ion Complexes, Supplement No. 1. London, The Chemical Society, p 482.
Slessor, K. N., and Tracey, A. S. (1971), *Can. J. Chem. 49*, 2874.
Sternhell, S. (1969), *Quart. Rev., Chem. Soc. 23*, 236.
Stothers, J. B. (1972), Carbon-13 NMR Spectroscopy, New York, N. Y., Academic Press: (a) pp 148–151, (b) p 197, (c) pp 279–289, (d) pp 348–362.
Teuwissen, B., Masson, P. L., Osinski, P., and Heremans, J. F. (1972), *Eur. J. Biochem. 31*, 239.
Vinogradov, S. N., and Linnell, R. H. (1971), Hydrogen Bonding, New York, N. Y., Van Nostrand Reinhold Co., pp 94–95.
Winkler, F. K., and Dunitz, J. D. (1971), *J. Mol. Biol. 59*, 169.
Yan, L. F., Momany, F. A., Hoffmann, R., and Scheraga, H. A. (1970), *J. Phys. Chem. 74*, 420.
Zalkin, A., Forrester, J. D., and Templeton, D. H. (1966), *J. Amer. Chem. Soc. 88*, 1810.

Fractionation of Mouse Myeloma Chromatin†

Edwin C. Murphy, Jr.,*‡ Stanton H. Hall,§ Judith H. Shepherd,¶ and Russell S. Weiser

ABSTRACT: Chromatin was isolated from several mouse myelomas and fractionated after shearing on both sucrose and glycerol gradients. The fractionation procedure resulted in the separation of two classes of chromatin as defined by their sedimentation properties and capacity for RNA synthesis *in vivo* and *in vitro*. The first class, slowly sedimenting chromatin, was composed of chromatin particles with widely varying template capacities as estimated with the RNA polymerase obtained from *Escherichia coli* and both the form II (nucleoplasmic) and form I (nucleolar) DNA-dependent RNA polymerases purified from a myeloma tumor. The second class, rapidly sedimenting chromatin, was heterogeneous with respect to size and uniformly unable to support RNA synthesis *in vitro*. Slowly sedimenting chromatin contained 10–20% of the total chromatin DNA and possessed >90% of the *in vitro* template activity. The validity of the *in vitro* assays for RNA synthesis as a method of estimating the fractionation of chromatin into functionally distinct classes was confirmed by the observation that newly synthesized RNA molecules were found selectively associated with slowly sedimenting chromatin *in vivo*. Analysis on polyacrylamide–sodium dodecyl sulfate gels revealed that rapidly sedimenting chromatin possessed two prominent high molecular weight nonhistone proteins which are absent in slowly sedimenting (template-active) chromatin. Conversely, four or more nonhistone proteins were selectively associated with the template-active chromatin. The capacity for specific interaction of DNA and chromosomal proteins was examined by reconstitution of dissociated chromatin. It was found that reconstituted chromatin, although not identical with native chromatin, retained a portion of its structural and functional heterogeneity.

Chromatin, the interphase form of chromosomes, is a complex of DNA, proteins, and RNA. In most cells, the major part of the genome is in the repressed state. Studies using RNA–DNA hybridization have suggested that only a minor yet tissue-specific fraction of the DNA sequences in chromatin (5–15%) is active in RNA synthesis and that the necessary elements for the control of tissue-specific RNA synthesis are retained in the isolated complex (Paul and Gilmour, 1968; Smith *et al.*, 1969; Huang and Huang, 1969; Hahn and Laird, 1971; Grouse *et al.*, 1972). Consequently, most studies on chromatin deal with material which is predominantly inactive.

One approach to the study of the relationship between the components of chromatin and its function as a template for RNA synthesis is to attempt the fractionation of chromatin into segments which are transcribed *in vivo* and those which are repressed. Electron microscopy has revealed that interphase chromatin is a mixture of electron-dense and diffuse regions. Radioautographic studies have established that the diffuse regions are template-active, whereas the condensed regions are not (Littau *et al.*, 1964, 1965). There have been several studies designed to separate the extended and condensed regions of chromatin. Frenster *et al.* (1963) reported the separation of sonicated thymocyte chromatin by centrifugation into a supernatant fraction with considerable

† From the Departments of Microbiology and Pathology, The University of Washington, Seattle, Washington 98105. *Received January 31, 1973.* Supported in part by U. S. Public Health Service Grants AM 08686 and CA 13600, American Cancer Society Grant NP-99C, and National Institutes of Health Training Grant 2-T01-CA05040.

‡ Present address: Department of Biology, The Johns Hopkins University, Baltimore, Md. 21218.

§ Postdoctoral Trainee in Experimental Pathology; supported by U. S. Public Health Service Grant GM-0100.

¶ Predoctoral Fellow supported by National Institutes of Health Grant 5-F01-GM-45030.